
THE FRACTAL DIMENSION OF AN OIL SPRAY

R. CASTREJÓN GARCÍA

*Instituto de Investigaciones Eléctricas
Av. Reforma 113, 62490 Cuernavaca, Morelos, México*

A. SARMIENTO GALÁN

*Instituto de Matemáticas, UNAM
Av. Universidad s/n, 62200 Chamilpa, Morelos, México
ansar@matcuer.unam.mx*

J. R. CASTREJÓN PITA and A. A. CASTREJÓN PITA

*Centro de Investigación en Energía, UNAM
Apdo. Postal 34, 62580 Temixco, Morelos, México*

Received September 12, 2002

Accepted October 2, 2002

Abstract

We study the fractal dimension of the contour of the liquid-gas interface in a spray. Our images include both the linking region and the break-up region, and are obtained with a high-resolution shadowgraph technique. This means that the images can then be subjected to an intensity filtering, equivalent to a threshold analysis, that enables the establishment of the fractal range.

Keywords: Fractality; Nonlinear Interactions; Interface Dynamics.

1. INTRODUCTION

The study of the geometric complexity in the break-up region of the liquid-gas interface in sprays represents a topic of special interest, due to the fact

that the physical process of atomization^a is intimately related to many commercial and technological applications.¹ The use of aerosol visualization

^aWe use here the common, albeit incorrect, sense for the word. According to its etymology, atom is an indivisible entity, and thus, to atomize really means to make indivisible, a meaning which is exactly the opposite to the intention when commonly used.

analysis includes fields as diverse as the application of pesticides and insecticides to crops, hand-held sprays for painting or drying, fuel injection in combustion engines, liquid fuel spraying in the power generation industry, spray coating of pharmaceutical products, nuclear core cooling and commercial filling processes, to mention just a few,^{2,3} and the studies are carried out with the efficient application of liquids, fuels or oils, in mind. In our study, the emphasis is set on the details of the relation between some properties of the fluid, like homogeneity or terminal speed, and the distance to the spray nozzle.

The use of shadowgraph images as a visualization tool is not new; their use in complexity studies however, has not been thoroughly exploited. Since our images are obtained with a high-resolution shadowgraph technique, they have proven specially pertinent for the implementation of the detailed analysis presented elsewhere for experiments in transport by fluids.⁴

2. EXPERIMENTAL SET-UP

Among the different optical techniques that are used for the study of particles, liquids or gases in motion, the shadowgraphy stands out as an inexpensive and powerful technique.⁵ Its main advantage is to highlight the relative refractive index of bodies, and thus to allow the visualization of objects that would be impossible to attain with the conventional photographic techniques. This is particularly useful when the objects to photograph are transparent instead of opaque, i.e. air and water, or transparent fluids with different refractive indexes.

In the shadowgraph technique, the object is illuminated from its back through an optical system designed specifically for such purposes. In this way, the light that strikes the photographic film is the one that passes through, without interacting with the object; the light that interacts with the object is absorbed or deviated aside due to a difference in its refractive index and does not influence the film. Figure 1 shows a schematic view of the shadowgraph system used for this work.

The atomization process occurs as a result of the interaction between the oil in its liquid state and the surrounding air, and involves several stages through which the oil becomes an aerosol. These stages can be clearly observed in any of the pictures. Initially, as soon as the oil is forced to leave the atomizer

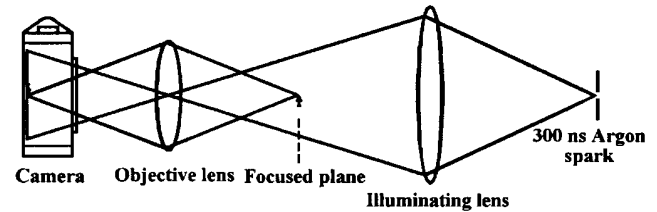


Fig. 1 Schematic view of the shadowgraph device used.

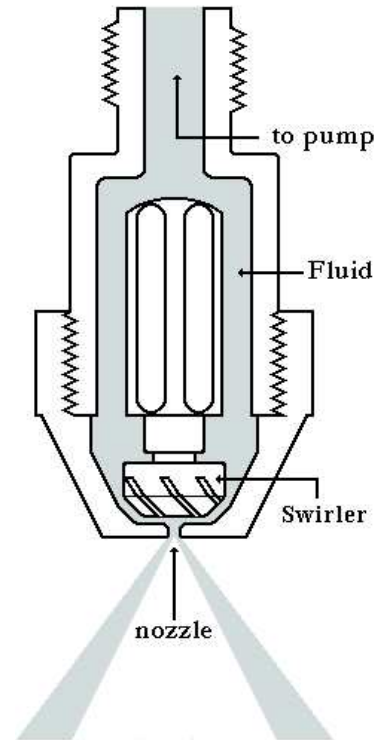


Fig. 2 Nozzle atomizer, a 1 mm ϕ orifice producing a 45° hollow cone.

nozzle with a velocity that has both axial and radial components, the fluid is turned into thin laminar waves that are gradually converted by the aerodynamic forces into thin ligaments. Downstream, these ligaments are broken up into a cloud of small droplets that continue to move with a terminal average velocity of several meters per second.

Our photographs correspond to the spray of transparent oil produced by a pressure swirl atomizer: the nozzle orifice is 1 mm in diameter and produces a hollow cone spray with an amplitude of 45° (Fig. 2). The atomization pressure, obtained with a common gear pump, is 4×10^5 Pa. The fluid is a blend of industrial oils designed to match the characteristics of diesel fuel which produces

an impressive and complex droplets formation spray.⁶

The measurement of the terminal speed was carried out with a technique preceding the Particle Image Velocimeter (PIV) based on a double photographic exposure. The break-up region is optically magnified (three times in our case) and the ISO 400 b&w professional film is imprinted by a double flash from an Argon jet stabilized spark gap which lasts for 300 ns and is shot again after 0.1 ms; this creates a double image whose characteristic and identifiable features are separated by a certain distance that, together with the time lapse between flashes and the optical magnification, allow for the determination of the droplets speed. The mean speed thus measured at the break-up region, 30 mm from the nozzle, has a value of 15.5 m/s. Although no magnification exists in the photographs used for this work, the type of film employed allows for a photographic magnification of up to 20 times without any

loss of sharpness. Finally, in order to analyze their structure, the photographs were digitalized with a resolution of 150 dpi in an eight-bit gray-scale comprising of 254 tonalities of gray.

3. MEASUREMENTS

We have used the well-known box-counting method to calculate the fractal dimension of the spray contour: a grid of size ε is superimposed on the black and white images and then, the boxes of this grid that intersect any part of the image are counted to provide the number N ; the process is repeated reducing the size of the grid and thus, the discrete function $N(\varepsilon)$ is generated. The initial size is usually a one-pixel grid⁷⁻⁹ and the number of pixels of size $1/\varepsilon$ is increased until the grid size reaches a certain previously determined value (this value is usually given by the smallest possible pixel size).

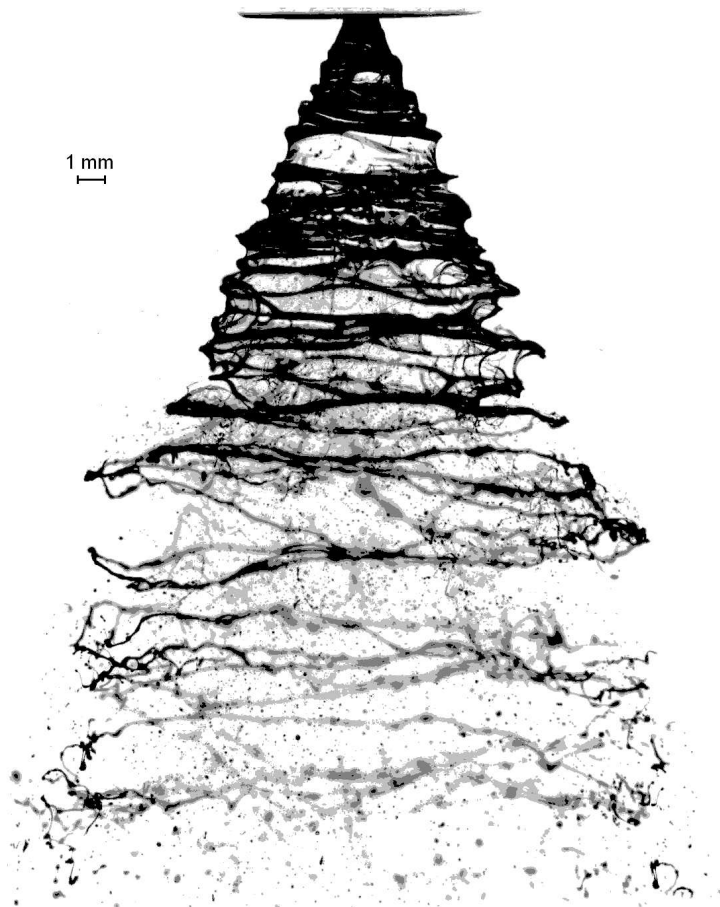


Fig. 3 Typical image obtained by the shadowgraph technique applied to an oil spray produced by the pressure swirl atomizer in Fig. 2.

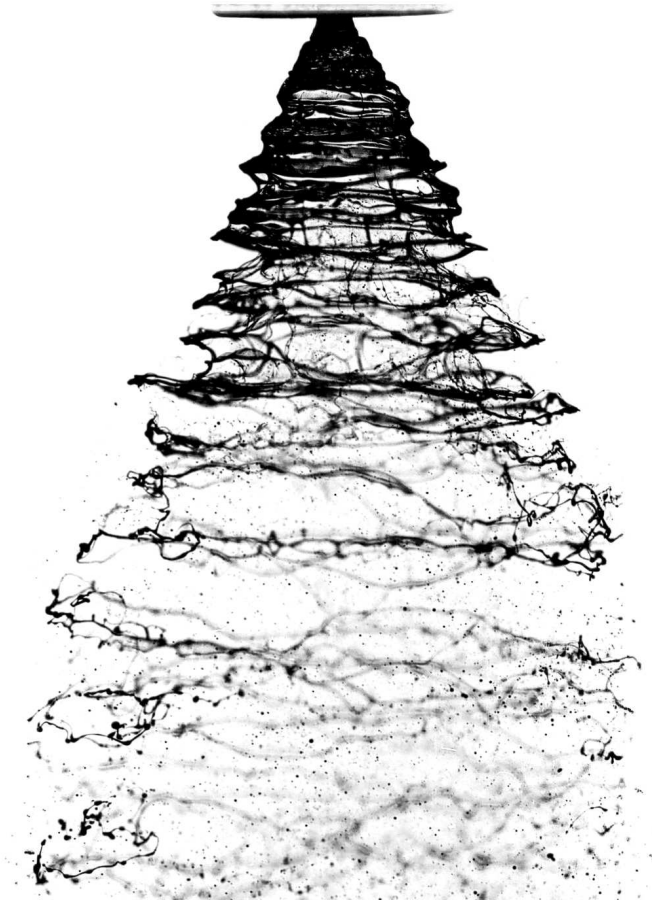


Fig. 4 Another typical image of the oil spray.

Finally, one is interested in the limit

$$D = \lim_{\varepsilon \rightarrow 0} \frac{\ln N(\varepsilon)}{\ln(1/\varepsilon)}$$

which defines the fractal dimension D . For the analysis of the contour of the oil aerosol, examples shown in Figs. 3 and 4, we varied the size of the grid from 1 to 1300 pixels (the longitude of the image in pixels) and 25 different images of the spray were taken under the same physical conditions; within the attainable accuracy, the corresponding results produce all the same value.

The box-counting method is designed for monochromatic images,^{8,10} and thus one has to be very careful when analyzing either color or varying intensity images. This is due to the fact that the features from the image whose intensity is below a certain value, called the threshold level, will be lost when transforming the image to a black and white one.⁴ In our case, this problem is represented by some parts of the image being less opaque than

others due to light extinction; some thin filaments are less opaque than their thicker similes. Even though every precaution was taken to adjust the depth of field to the size of the spray, some small contribution to this intensity problem may arise from a lack of perfect focusing. To avoid complications arising from this difficulty, our analysis was carried out by filtering each image at every gray tonality from the zeroth to the 254th level of the digitalized images, i.e. the first filter takes into account the black parts only, and then the intensity is diminished one digital step to incorporate the less opaque features of every image gradually. If this filtering process is not carried out, the simple transformation of the images to black and white ones produces the equivalent of filtering every image at half its maximum intensity value (Figs. 5 and 6). However, as shown in the following section, the filtering process just described reveals the rich fractal structure of the oil spray over a much wider range of intensity values or gray tonalities.

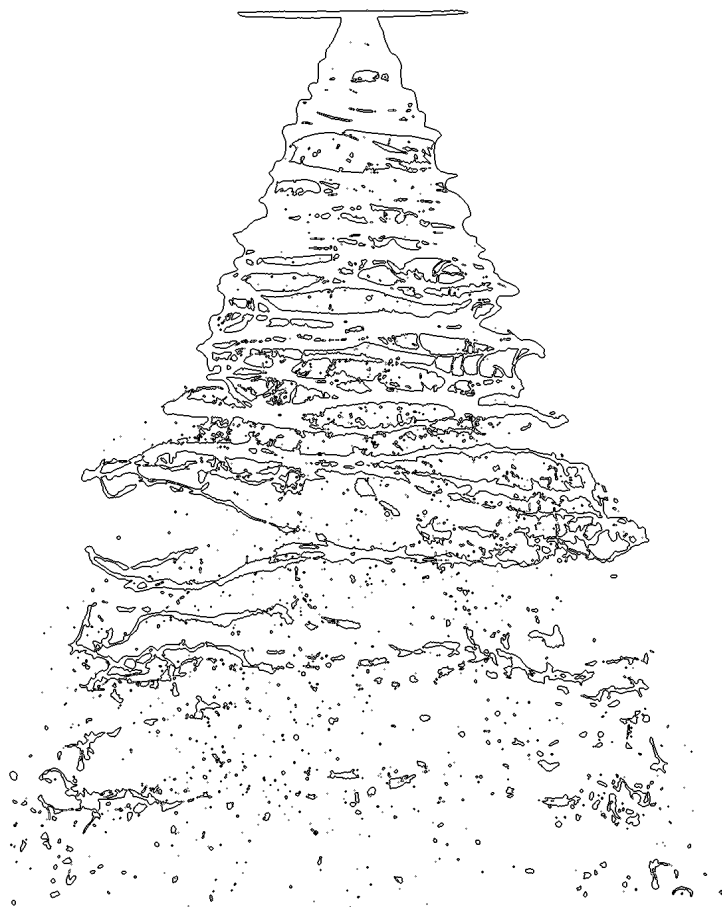


Fig. 5 Image showing the resulting contour of the spray in Fig. 3 when the filtering is done at half the maximum intensity value.

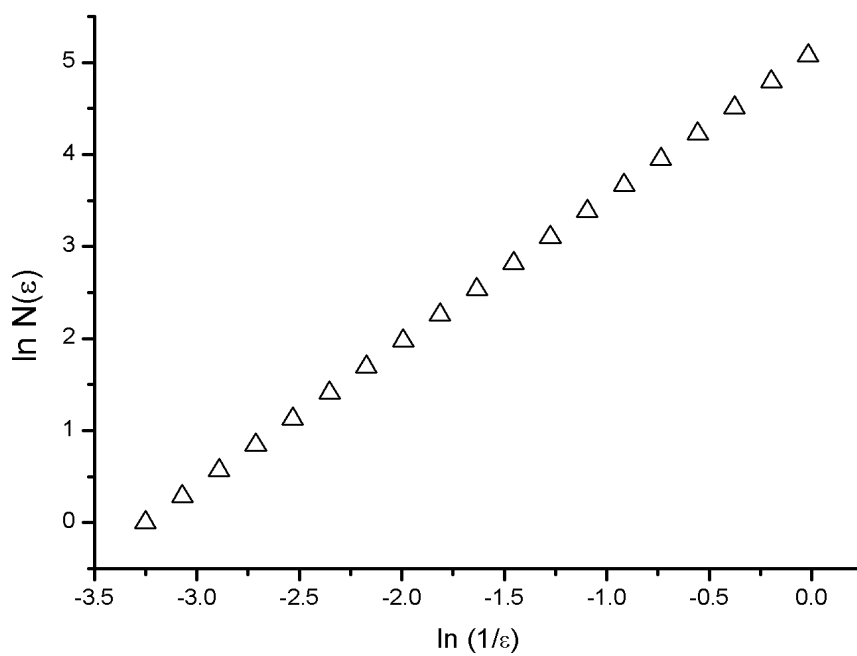


Fig. 6 Results from the box-counting method at half-intensity filtering.

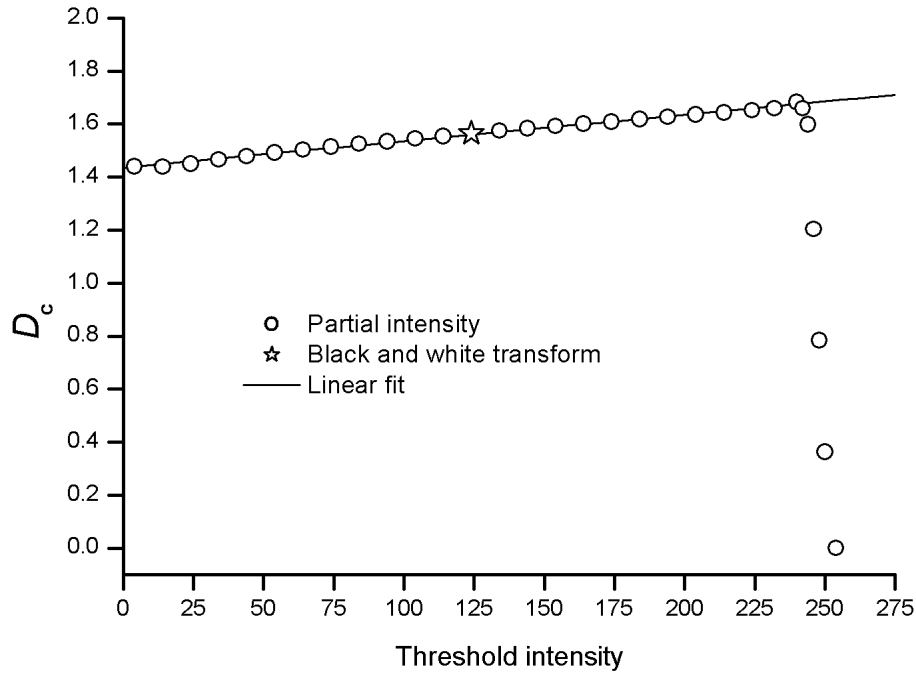


Fig. 7 Intensity threshold dependence of the fractal dimension.

4. RESULTS

Using the Intersection Theorem,⁴ we find that the fractal dimension of the contour of the oil spray when the images are only filtered at half their maximum intensity is 2.57 ± 0.03 with a linear correlation coefficient of 0.98; the result is illustrated in Fig. 6. The whole spectrum of the fractal dimension of the contour however, is shown in Fig. 7, where the diameter of the open circles indicates the uncertainty at each intensity value and corresponds to the standard deviation of the data in all the 25 analyzed photographs. To illustrate the fractal structure and the self-similarity of the contour at different intensities, the graph in Fig. 7 includes the fractal dimension value obtained from the filtering process starting at the level in which the image becomes a single black rectangle up to the level of a single white one. The graph displays the fractal structure for the whole digital intensity range; a small star indicates the already mentioned fractal dimension at half-intensity filtering (126th digital level). A linear fit with a correlation coefficient of 0.997 is also shown, the slope and ordinate are: $(9.969 \pm 0.154) \times 10^{-4}$ and 1.436 ± 0.002 , respectively. After the 249th digital level, the filtering leaves no tractable structure in the image; the gradual decay of the fractal dimension observed in Fig. 7, from the 249th to the

254th digital level of gray, is therefore due to a tenuous gray intensity present in the background of our photographs.

5. CONCLUSIONS

The shadowgraph technique allows us to obtain high-definition images of the whole oil spray, which are ideal for the analysis of the dynamics of the aerosol and even of its smallest details, since the image can be magnified several tenth times without noticeable loss of sharpness; a higher density of dots is equivalent to a smaller pixel size which enables the analysis of smaller regions in the image.

For complexity studies of similar systems through fractal dimension analysis¹⁰, it may be possible to use b&w photographs since the strong linear relation between intensity and threshold assures the existence of an interval (centered at the b&w intensity value) where the fractal dimension will remain linear in relation to the intensity. However, the analysis carried out for the contour intensity clearly indicates that, in this and similar cases, it is not suitable to directly digitalize the images in a purely black and white format, since then all the rich structural information contained in the gray tonalities is irremediably lost.

ACKNOWLEDGMENTS

This work has been partially supported by the IIE (México), and DGAPA-UNAM (project IN101100). AACCP acknowledges financial support from DGEP-UNAM.

REFERENCES

1. W. X. Zhou and Z. H. Yu, *Phys. Rev.* **E63**, 016302 (2000).
2. R. C. Baker, *Flow Measurement Handbook* (Cambridge University Press, 2000).
3. Y. Wen-Jei, *Handbook of Flow Visualization* (Taylor & Francis Ed., Michigan, 1989).
4. R. R. Prasad and K. R. Sreenivasan, *Phys. Fluids*, **A2**(5), 792 (1990).
5. A. R. Jones, *A Review of Drop Size Measurement. The Application of Techniques to Dense Fuel Sprays*, Vol. 3 (Progress in Energy and Combustion Sciences, 1977).
6. N. Brombrowski, *J. Agric. Eng. Res.* **23**, 37 (1961).
7. J. R. Castrejón Pita, A. Sarmiento Galán and R. Castrejón García, *Fractals* **10**(4), 429 (2002).
8. M. Nežadal and O. Zmeskal, *Harmonic and Fractal Image Analyzer* (code) (2001), e-Archive: <http://www.fch.vutbr.cz/lectures/imagesci>
9. U. Shavit and N. Chigier, *Fractals*, **2**, 2 (1994).
10. K. T. Alligood, T. D. Sauer and J. A. Yorke, *Chaos: An Introduction to Dynamical Systems* (Springer Press, New York, 1996), pp. 172–180.